Modal Analysis of Homogeneous Optical Waveguides by Boundary Integral Method

Lei Wang * J. Allen Cox † Avner Friedman *

January 23, 1997

Abstract

The optical field in a weakly guiding homogeneous waveguide satisfies scalar Helmholtz equations in both the core and cladding, and transmission conditions on the boundary. The transverse wavenumbers of the two scalar Helmholtz equations for the core and cladding are different and both of them depend on the propagation constants in the longitudinal direction of the waveguide. Two different systems of boundary integral equations are derived for the numerical solutions of the discrete propagation constants; one of them is in the form of Fredholm integral equations of the second kind and the other is a "mixed" first and second kind. A Nyström algorithm is used to solve the boundary integral equations numerically. The numerical results show that the two boundary integral formulations are both very efficient in the numerical simulations of homogeneous waveguides. But the second kind is more advantageous because it controls spurious modes better.

1 Introduction

In this paper, we apply a Nyström algorithm and the boundary integral method to the numerical solution of homogeneous (step-index) dielectric waveguides.

The boundary integral method[1, 2] translates a boundary value problem of partial differential equation into a system of integral equations on the boundaries; thus one only needs to compute unknowns on the boundaries at first. The solution for the whole space can be expressed in terms of the solution on the boundaries. The method is well suited for dealing with homogeneous regions, and has thus been used to investigate the propagation characteristics of the step-index dielectric waveguides by several authors[3, 4, 5]. However, two improvements can be done for the boundary integral method.

*Institute for Mathematics and Its Applications, University of Minnesota, 206 Church Street S.E., Minneapolis, MN 55455

†Honeywell Technology Center, Honeywell Inc., 3660 Technology Dr., Minneapolis, MN 55418

First, in [3, 4, 5], the boundary integral equations are discretized by the point-matching method (also called the collocation method) in which the boundary is approximated by a polygon and each of the matrix elements of the resulting linear system is a simple integral over one or two sides of the polygon. This method is superior to the Galerkin method in numerical efficiency, because the latter requires a double integration for each of the matrix elements[6]. Nevertheless, for two-dimensional problems (or one-dimensional integral equations), the most efficient method is the Nyström method in which only an evaluation of the kernel function is needed for each of the matrix elements[7]. More importantly, for two-dimensional problems with closed boundaries, the global approximations via trigonometric polynomials are available for the numerical quadratures of the boundary integrals[7]. The corresponding numerical integration rules converge exponentially, i.e., the error is of order of $O(\exp(-\sigma/h))$ where h is the mesh size and σ is some positive constant. This improvement is very important for the numerical computation of a multimode dielectric waveguide where the waveguide frequency is much larger than 1.

Second, we are not aware any work which uses the boundary integral equation of the second kind for this problem. As we will show in this paper, a boundary integral equation of the second kind is preferable to the formulation in [3, 4, 5] because of its better control of spurious modes.

We deal with the weakly guiding waveguides (scalar wave equations) only. But the method (including the derivation of the second kind integral equation) can be easily extended to strongly guiding waveguides (vector wave equations) and waveguide arrays ([4] and [5] deal with vector wave equations only). The formulation of the boundary value problem is given in Section 2. The Nyström method and a special treatment for non-smooth boundaries are presented in Sections 3 and 4 respectively. A modified algorithm for the computation of multimode waveguides is described in Section 5. Numerical examples of circular and rectangular step-index waveguides are described in Section 6.

2 Mathematical Formulation

Consider a homogeneous dielectric cylinder of arbitrary cross section cladded by another homogeneous medium which extends to infinity, as shown in Figure 1. The waveguide is

uniform in the Z direction. We denote the refractive index in the core (Ω) by n_1 and the refractive index in the cladding ($\Omega^c = \mathbb{R}^2 \setminus \bar{\Omega}$) by n_2 and assume that $n_1 > n_2$.

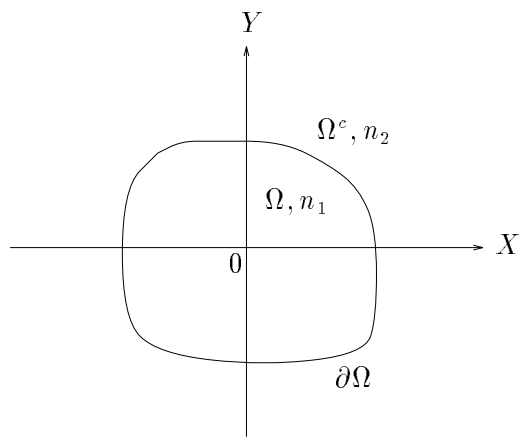

Figure 1: A homogeneous waveguide.

For the weakly guiding waveguides which satisfy $(n_1 - n_2)/n_1 \ll 1$, the electric and magnetic fields of each guiding mode can be modeled by the scalar Helmholtz equations [8]:

$$\nabla^2\psi + (n_1^2k^2 - \beta^2)\psi = 0 \quad \text{in } \Omega, \tag{1a}$$

$$\nabla^2\psi + (n_2^2k^2 - \beta^2)\psi = 0 \quad \text{in } \Omega^c, \tag{1b}$$

$$\psi \text{ and its normal derivative are continuous across } \partial\Omega, \tag{1c}$$

$$\psi(X,Y) \to 0 \text{ as } \sqrt{X^2+Y^2} \to \infty, \tag{1d}$$

where $\psi = \psi(X,Y)$ is any transverse component of the electric or magnetic field, k is the wavenumber in free space, and β is the propagation constant in the Z direction. By introducing a normalized propagation constant $P = (\beta^2 - n_2^2k^2)/(n_1^2 - n_2^2)k^2$ and normalized coordinates $x = X/\rho, y = Y/\rho$ where ρ represents the size of the waveguide core cross section, we get the following eigenvalue problem:

$$\nabla^2\psi + V^2(1-P)\psi = 0 \quad \text{in } \Omega, \tag{2a}$$

$$\nabla^2\psi - V^2P\psi = 0 \quad \text{in } \Omega^c, \tag{2b}$$

$$\psi \text{ and } \frac{\partial\psi}{\partial n} \text{ are continuous across } \partial\Omega, \tag{2c}$$

$$\psi(x,y) \to 0 \text{ as } \sqrt{x^2+y^2} \to \infty, \tag{2d}$$

where $V = \rho k(n_1^2 - n_2^2)^{1/2}$ is the waveguide frequency, $\partial/\partial n = \mathbf{n}\cdot\nabla$ and $\mathbf{n}$ is the unit vector

in the outward normal direction to $\partial\Omega$. For guided modes, we have $n_2 k < \beta < n_1 k$ or $0 < P < 1$.

Using the *Green's Third Identity*, the field ψ inside and outside the core can be expressed as boundary integrals by means of the fundamental solutions:

$$\psi(\mathbf{r}) = -\int_{\partial\Omega} \frac{\partial G_1(\mathbf{r},\mathbf{r}')}{\partial n'}\psi(\mathbf{r}')dl' + \int_{\partial\Omega} G_1(\mathbf{r},\mathbf{r}')\frac{\partial\psi(\mathbf{r}')}{\partial n'}dl', \quad \text{in } \Omega, \tag{3a}$$

$$\psi(\mathbf{r}) = \int_{\partial\Omega} \frac{\partial G_2(\mathbf{r},\mathbf{r}')}{\partial n'}\psi(\mathbf{r}')dl' - \int_{\partial\Omega} G_2(\mathbf{r},\mathbf{r}')\frac{\partial\psi(\mathbf{r}')}{\partial n'}dl', \quad \text{in } \Omega^c, \tag{3b}$$

where $\mathbf{r} = (x, y)$, n' and l' denote the local coordinates in the normal and tangential directions on the boundary. Here $G_1(\mathbf{r},\mathbf{r}')$ and $G_2(\mathbf{r},\mathbf{r}')$ are the fundamental solutions of the Helmholtz equations in the medium n_1 and the medium n_2, respectively, that is,

$$\nabla^2 G_l(\mathbf{r},\mathbf{r}') + h_l^2 G_l(\mathbf{r},\mathbf{r}') = -\delta(|\mathbf{r}-\mathbf{r}'|), \quad l = 1, 2, \tag{4}$$

where $h_1 = V(1-P)^{1/2}$ and $h_2 = -iVP^{1/2}$. For our case of the two-dimensional space $\mathbb{R}^2$, G_1 and G_2 are the Hankel functions of the second kind of order zero[1]:

$$G_l(\mathbf{r},\mathbf{r}') = \frac{1}{4i}H_0^{(2)}(h_l|\mathbf{r}-\mathbf{r}'|), \quad l = 1, 2. \tag{5}$$

We note that for real P, $G_2(\mathbf{r},\mathbf{r}') \to 0$ as $|\mathbf{r}-\mathbf{r}'| \to \infty$.

In (3a) and (3b), let $\mathbf{r}$ go to the boundary and note that the double layer potentials $\int_{\partial\Omega} \frac{\partial G_l}{\partial n'}\psi(\mathbf{r}')dl'$ have jumps of $-\psi(\mathbf{r})/2$ and $\psi(\mathbf{r})/2$ for $l = 1$ and $l = 2$ respectively. In the limit, we get a boundary integral formulation of the eigenvalue problem (2a)-(2d),

$$\frac{1}{2}\psi(\mathbf{r}) + \int_{\partial\Omega} \frac{\partial G_1(\mathbf{r},\mathbf{r}')}{\partial n'}\psi(\mathbf{r}')dl' - \int_{\partial\Omega} G_1(\mathbf{r},\mathbf{r}')\phi(\mathbf{r}')dl' = 0, \quad \mathbf{r} \in \partial\Omega, \tag{6a}$$

$$\frac{1}{2}\psi(\mathbf{r}) - \int_{\partial\Omega} \frac{\partial G_2(\mathbf{r},\mathbf{r}')}{\partial n'}\psi(\mathbf{r}')dl' + \int_{\partial\Omega} G_2(\mathbf{r},\mathbf{r}')\phi(\mathbf{r}')dl' = 0, \quad \mathbf{r} \in \partial\Omega. \tag{6b}$$

where $\phi(\mathbf{r}) = \frac{\partial\psi}{\partial n}(\mathbf{r})$. This system (which is derived in [3]) is a system of integral equations for the unknowns ψ and ϕ. It is not the second kind, and therefore its solution cannot be justified on rigorous mathematical arguments.

To derive boundary integral equations of the second kind, we first add up (6a) and (6b) to get

$$\psi(\mathbf{r}) - \int_{\partial\Omega} \frac{\partial}{\partial n'}(G_2 - G_1)\psi(\mathbf{r}')dl' + \int_{\partial\Omega}(G_2 - G_1)\phi(\mathbf{r}')dl' = 0, \quad \mathbf{r} \in \partial\Omega. \tag{7a}$$

[1] G_1 and G_2 can also be taken as the Hankel functions of the first kind of order zero, then $h_2 = iVP^{1/2}$.

Next, we take the normal derivatives of (3a) and (3b) and let $\mathbf{r}$ go to the boundary. The normal derivatives of the single layer potentials, $\frac{\partial}{\partial n}\int_{\partial\Omega} G_l \frac{\partial \psi}{\partial n'}(\mathbf{r}')dl'$, have jumps of $\psi(\mathbf{r})/2$ and $-\psi(\mathbf{r})/2$ for $l=1$ and $l=2$ respectively. But the normal derivatives of the double layer potentials, $\frac{\partial}{\partial n}\int_{\partial\Omega} \frac{\partial G_l}{\partial n'}\psi(\mathbf{r}')dl'$, are continuous across the boundary (cf. [9]). Consequently, by adding the limit equations we get

$$\phi(\mathbf{r}) - \int_{\partial\Omega} \frac{\partial^2}{\partial n \partial n'}(G_2 - G_1)\psi(\mathbf{r}')dl' + \int_{\partial\Omega} \frac{\partial}{\partial n}(G_2 - G_1)\phi(\mathbf{r}')dl' = 0, \quad \mathbf{r} \in \partial\Omega. \tag{7b}$$

(7a) and (7b) form a system of boundary integral equations of the second kind. The idea of deriving a system of boundary integral equations of the second kind, in the context of computing the electric potential for a macromolecule, has been used in [10]. For future reference we refer to (6a)-(6b) as the first method and to (7a)-(7b) as the second method.

In (6a)-(7b), there are four types of kernels: $G_l(\mathbf{r},\mathbf{r}')$, $\frac{\partial G_l}{\partial n'}(\mathbf{r},\mathbf{r}')$, $\frac{\partial(G_2-G_1)}{\partial n}(\mathbf{r},\mathbf{r}')$ and $\frac{\partial^2(G_2-G_1)}{\partial n \partial n'}(\mathbf{r},\mathbf{r}')$. We note that except for $G_l(\mathbf{r},\mathbf{r}')$ which is weakly singular[2], all other kernels are continuous for all $\mathbf{r},\ \mathbf{r}' \in \partial\Omega$. (Note that the functions $\frac{\partial^2 G_l}{\partial n \partial n'}$ are singular.) The Nyström method concerns with the discretizations of the four associated integral operators, and it is presented in the next section.

3 Nyström Method

Following [7], we assume that the boundary $\partial\Omega$ is analytic and can be represented in the parametric form:

$$\mathbf{r}(t) = (x(t), y(t)), \qquad 0 \le t \le 2\pi, \tag{8}$$

where $x(t), y(t)$ are analytic functions with 2π periodicity. Then

$$S_l(t,\tau) \equiv G_l \frac{dl'}{d\tau} = \frac{1}{4i} f_1(\tau) H_0^{(2)}(h_l R), \tag{9a}$$

$$D_l(t,\tau) \equiv \frac{\partial G_l}{\partial n'}\frac{dl'}{d\tau} = \frac{i h_l}{4} f_2(\tau,t) H_1^{(2)}(h_l R), \tag{9b}$$

$$D'(t,\tau) \equiv \frac{\partial(G_2 - G_1)}{\partial n}\frac{dl'}{d\tau} = \frac{i}{4}\frac{f_2(t,\tau) f_1(\tau)}{f_1(t)}[h_2 H_1^{(2)}(h_2 R) - h_1 H_1^{(2)}(h_1 R)], \tag{9c}$$

$$\begin{aligned} T(t,\tau) \equiv \frac{\partial^2(G_2 - G_1)}{\partial n \partial n'}\frac{dl'}{d\tau} = \frac{-i}{4 f_1(t)} \Big\{ & f_3(t,\tau)[h_2 H_1^{(2)}(h_2 R) - h_1 H_1^{(2)}(h_1 R)] \\ & + f_2(t,\tau) f_2(\tau,t)[h_2^2 H_2^{(2)}(h_2 R) - h_1^2 H_2^{(2)}(h_1 R)] \Big\}, \end{aligned} \tag{9d}$$

[2] It is singular at $r = r'$, but the associate integral operator is bounded.

where

$$
\begin{aligned}
f_1(t) &= \sqrt{[x'(t)]^2 + [y'(t)]^2}, \\
f_2(t,\tau) &= \frac{y'(t)[x(t)-x(\tau)] - x'(t)[y(t)-y(\tau)]}{R(t,\tau)}, \\
f_3(t,\tau) &= \frac{y'(t)y'(\tau) + x'(t)x'(\tau)}{R(t,\tau)}, \\
R = R(t,\tau) &= \{[x(t)-x(\tau)]^2 + [y(t)-y(\tau)]^2\}^{1/2}.
\end{aligned}
$$

By definition $H_n^{(2)}(z) = J_n(z) - iY_n(z)$ and the Neumann function $Y_n(z)$ is given by

$$
\begin{aligned}
Y_n(z) \;=\; & \frac{2}{\pi}\left(\ln\frac{z}{2} + \gamma\right) J_n(z) - \frac{1}{\pi}\sum_{p=0}^{n-1}\frac{(n-1-p)!}{p!}\left(\frac{2}{z}\right)^{n-2p} \\
& -\frac{1}{\pi}\sum_{p=0}^{\infty}\frac{(-1)^p}{p!(n+p)!}\left(\frac{z}{2}\right)^{n+2p}\left(\sum_{m=1}^{p+n}\frac{1}{m} + \sum_{m=1}^{p}\frac{1}{m}\right), \qquad (10)
\end{aligned}
$$

where $\gamma = 0.577215...$ is the Euler's constant. It can be seen that the kernel $S_l(t,\tau)$ is weakly singular. The kernels $D_l(t,\tau)$, $D'(t,\tau)$ and $T(t,\tau)$ are continuous, but none of them is analytic. Because the Neumann function $Y_n(z)$ has logarithmic singularity at $z = 0$, the derivatives (not necessarily the first order) of $D_l(t,\tau)$, $D'(t,\tau)$ and $T(t,\tau)$ fail to be continuous at $t = \tau$.

It is advantageous to separate the logarithmic parts from the kernels [7] as follows:

$$S_l(t,\tau) = S_{l1}(t,\tau)\ln\left(4\sin^2\frac{t-\tau}{2}\right) + S_{l2}(t,\tau), \qquad (11a)$$

$$D_l(t,\tau) = D_{l1}(t,\tau)\ln\left(4\sin^2\frac{t-\tau}{2}\right) + D_{l2}(t,\tau), \qquad (11b)$$

$$D'(t,\tau) = D'_1(t,\tau)\ln\left(4\sin^2\frac{t-\tau}{2}\right) + D'_2(t,\tau), \qquad (11c)$$

$$T(t,\tau) = T_1(t,\tau)\ln\left(4\sin^2\frac{t-\tau}{2}\right) + T_2(t,\tau), \qquad (11d)$$

where $S_{l1}, D_{l1}, D'_1, T_1$ and $S_{l2}, D_{l2}, D'_2, T_2$ are all analytic. The functions $S_{l1}, D_{l1}, D'_1, T_1$ are given by

$$S_{l1}(t,\tau) \;=\; -\frac{1}{4\pi}f_1(\tau)J_0(h_l R), \qquad (12a)$$

$$D_{l1}(t,\tau) \;=\; \frac{h_l}{4\pi}f_2(\tau,t)J_1(h_l R), \qquad (12b)$$

$$D'_1(t,\tau) \;=\; \frac{1}{4\pi}\frac{f_2(t,\tau)f_1(\tau)}{f_1(t)}[h_2 J_1(h_2 R) - h_1 J_1(h_1 R)], \qquad (12c)$$

$$T_1(t,\tau) = \frac{-1}{4\pi f_1(t)}\{f_3(t,\tau)[h_2 J_1(h_2 R) - h_1 J_1(h_1 R)] + f_2(t,\tau) f_2(\tau,t)[h_2^2 J_2(h_2 R) - h_1^2 J_2(h_1 R)]\}, \tag{12d}$$

and $S_{l2}, D_{l2}, D_2', T_2$ can be derived from (11a)-(11d).

To discretize the integral equations, we take an equidistant set of knots $t_j = \pi j/N, j = 0, 1, ..., 2N-1$, on the boundary $\partial\Omega$. The integral $\int_0^{2\pi} S_l(t,\tau)\psi(\tau)d\tau$, for example, is approximated by the quadrature rule

$$\int_0^{2\pi} \ln\left(4\sin^2\frac{t-\tau}{2}\right) S_{1l}(t,\tau)\psi(\tau)d\tau \approx \sum_{j=0}^{2N-1} R_j^{(N)}(t) S_{1l}(t,t_j)\psi(t_j), \quad 0 \le t \le 2\pi, \tag{13}$$

where

$$R_j^{(N)}(t) = -\frac{2\pi}{N}\sum_{m=1}^{N-1}\frac{1}{m}\cos m(t-t_j) - \frac{\pi}{N^2}\cos N(t-t_j), \tag{14}$$

and the trapezoidal rule

$$\int_0^{2\pi} S_{l2}(t,\tau)\psi(\tau)d\tau \approx \frac{\pi}{N}\sum_{j=0}^{2N-1} S_{l2}(t,t_j)\psi(t_j). \tag{15}$$

These two quadrature formulas have errors that are in the order of O(exp(-σN)) where $2N$ is the knot number and σ is equal to half of the width of a parallel strip in the complex plane into which the (real analytic) integrands can be analytically continued (see p.69 of [7]). With the help of the two quadrature rules (13) and (15), the two systems of integral equations (6a)-(6b) and (7a)-(7b) are converted to two linear algebraic systems:

$$\begin{pmatrix} \frac{1}{2}\mathbf{I} + \mathbf{D}_1 & -\mathbf{S}_1 \\ \frac{1}{2}\mathbf{I} - \mathbf{D}_2 & \mathbf{S}_2 \end{pmatrix} \begin{pmatrix} \Psi \\ \Phi \end{pmatrix} = 0, \tag{16}$$

and

$$\begin{pmatrix} \mathbf{I} - (\mathbf{D}_2 - \mathbf{D}_1) & \mathbf{S}_2 - \mathbf{S}_1 \\ -\mathbf{T} & \mathbf{I} + \mathbf{D}' \end{pmatrix} \begin{pmatrix} \Psi \\ \Phi \end{pmatrix} = 0, \tag{17}$$

where the two vectors Ψ and Φ are

$$\Psi = (\psi(t_0), \psi(t_1), ..., \psi(t_{2N-1}))', \tag{18}$$

$$\Phi = (\phi(t_0), \phi(t_1), ..., \phi(t_{2N-1}))', \tag{19}$$

$\mathbf{I}$ is the unit matrix and the elements of the other matrices are given by

$$\mathbf{S}_l(i,j) = S_{l1}(t_i,t_j)R_j^{(N)}(t_i) + \frac{\pi}{N}S_{l2}(t_i,t_j), \qquad l = 1,2, \tag{20a}$$

$$\mathbf{D}_l(i,j) = D_{l1}(t_i,t_j)R_j^{(N)}(t_i) + \frac{\pi}{N}D_{l2}(t_i,t_j), \qquad l = 1,2, \tag{20b}$$

$$\mathbf{D}'(i,j) = D'_1(t_i,t_j)R_j^{(N)}(t_i) + \frac{\pi}{N}D'_2(t_i,t_j), \tag{20c}$$

$$\mathbf{T}(i,j) = T_1(t_i,t_j)R_j^{(N)}(t_i) + \frac{\pi}{N}T_2(t_i,t_j). \tag{20d}$$

To have non-zero solutions for (Ψ, Φ), the determinants of the coefficient matrices (denoted by Q) in (16) and (17) have to vanish, which give us the eigenvalue equations for P:

$$|Q(P)| \equiv \det Q(P) = 0. \tag{21}$$

Note that the above equation is complex, but the physically correct eigenvalues P are real.

This discretization method is called Nyström or quadrature method in the sense that the straightforward approximations of the integrals by quadrature formulas (13) and (15) are used.

4 Boundary With Corners

If the boundary $\partial\Omega$ has corners, then $S_{l1}, D_{l1}, D'_1, T_1$ and $S_{l2}, D_{l2}, D'_2, T_2$ as well as ψ and ϕ are no longer analytic functions, and the exponential convergence cannot be obtained. A uniform mesh has to be replaced by a graded mesh for high order convergence. This should be done through a change of variable $t = w(s)$ in such a way that the derivatives of $w(s)$ vanishes up to a certain order $p-1$ at the corners [7]. The quadrature rules (13) and (15) can then be used for the transformed integrals. A fast convergence can be realized if p is large enough [7].

Let us consider a rectangle. Figure 2 shows the coordinate system and waveguide dimension. The boundary can be divided into five intervals in the angle s: $[0,\alpha], (\alpha, \pi-\alpha], (\pi-\alpha, \pi+\alpha], (\pi+\alpha, 2\pi-\alpha], (2\pi-\alpha, 2\pi)$. The function $t = w(s)$ can be defined piecewise as

$$w(s) = 2\alpha_2 \frac{U^p(s+\alpha_1-c)}{U^p(s+\alpha_1-c) + U^p(\alpha_1+c-s)} - \alpha_2 + c, \tag{22}$$

where $p(>2)$ is a positive integer,

$$U(s) = \left(\frac{1}{2} - \frac{1}{p}\right)\left(\frac{s-\alpha_1}{\alpha_1}\right)^3 + \frac{s-\alpha_1}{p\alpha_1} + \frac{1}{2}, \tag{23}$$

and

$$c = 0,\ \pi/2,\ \pi,\ 3\pi/2,\ 2\pi, \tag{24}$$

$$\alpha_1 = j_1\pi/N,\ \pi/2 - j_1\pi/N,\ j_1\pi/N,\ \pi/2 - j_1\pi/N,\ j_1\pi/N, \tag{25}$$

$$\alpha_2 = \alpha,\ \pi/2 - \alpha,\ \alpha,\ \pi/2 - \alpha,\ \alpha, \tag{26}$$

for the five intervals, respectively; here $j_1 = [\alpha N/\pi]$. A typical graph of $w(s)$ is given in Figure 3. By expanding $w(s)$ into Taylor series at $s = j_1\pi/N, \pi - j_1\pi/N, \pi + j_1\pi/N, 2\pi - j_1\pi/N$, it can be proved that the derivatives of $w(s)$ vanish up to the order $p-1$ at these points which correspond to the four corners in the t variable.

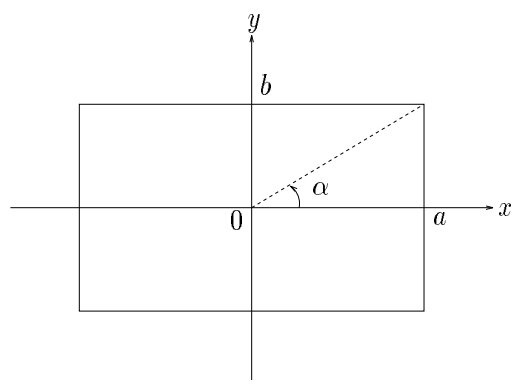

Figure 2: A rectangular waveguide.

Since a rectangle is symmetric with regard to the $x-$axis and $y-$axis, the electromagnetic field of a single guided mode should be either symmetric or anti-symmetric with respect to the $x-$axis and $y-$axis. Therefore, only a quarter region of the total waveguide cross section needs to be considered in the numerical computation, and all the guided modes can be divided into four groups designated by $(l_x, l_y) = (0,0)$, $(0,1)$, $(1,0)$, $(1,1)$, respectively. Here $l_x = 0$ (or 1) means the field is symmetric (or anti-symmetric) with regard to the $x-$axis, and same holds for l_y.

Using the angle variable transformation $t = w(s)$ and the symmetry of the rectangle, we once again arrive at the linear systems (16) and (17) where

$$\Psi = (\bar{\psi}(s_{l_x}), ..., \bar{\psi}(s_{j_1-1}), \bar{\psi}(s_{j_1+1}), ..., \bar{\psi}(s_{N/2-l_y}))', \tag{27}$$

$$\Phi = (\bar{\phi}(s_{l_x}), ..., \bar{\phi}(s_{j_1-1}), \bar{\phi}(s_{j_1+1}), ..., \bar{\phi}(s_{N/2-l_y}))', \tag{28}$$

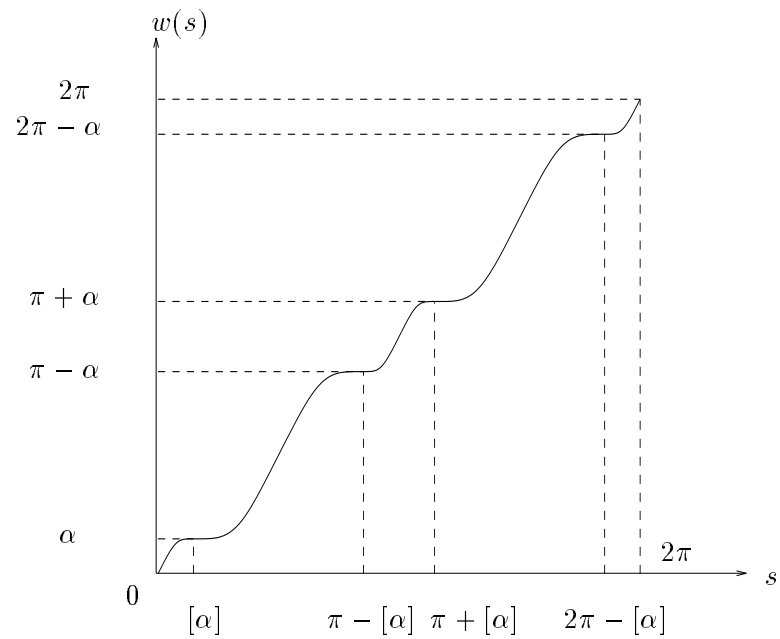

Figure 3: The function $w(s)$, here $[\alpha] = j_1\pi/N$.

and

$$\begin{aligned}
\mathbf{S}_l(i,j) \;=\; & w'(s_j)[S_{l1}(s_i,s_j)R_j^{(N)}(s_i) + \frac{\pi}{N}S_{l2}(s_i,s_j)] \\
& +(-1)^{l_y}w'(s_{N-j})[S_{l1}(s_i,s_{N-j})R_{N-j}^{(N)}(s_i) + \frac{\pi}{N}S_{l2}(s_i,s_{N-j})] \\
& +(-1)^{l_x+l_y}w'(s_{N+j})[S_{l1}(s_i,s_{N+j})R_{N+j}^{(N)}(s_i) + \frac{\pi}{N}S_{l2}(s_i,s_{N+j})] \\
& +(-1)^{l_x}w'(s_{2N-j})[S_{l1}(s_i,s_{2N-j})R_{2N-j}^{(N)}(s_i) + \frac{\pi}{N}S_{l2}(s_i,s_{2N-j})], \qquad (29)
\end{aligned}$$

for $i,j = l_x, ..., j_1-1, j_1+1, N/2-l_y$, where $s_j = j\pi/N, w' = dw/ds, \bar{\psi}(s_j) = \psi(w(s_j))$, and $\bar{\phi}(s_j) = \phi(w(s_j))$. For $j = 0, N/2$, the second and fourth terms on the right hand side of (29) should be dropped. Note that if ψ is anti-symmetric with respect to the x-axis ($l_x = 1$), it is zero on the x-axis, and so there is no need to include $\bar{\psi}(s_0)$ in the computation. The symmetry property of ϕ is as same as that of ψ. Therefore, the first knot should be $s_1 = \pi/N$ in this case. In the symmetric case ($l_x = 0$), we start with $s_0 = 0$. Thus in both cases, the first knot is s_{l_x}. Similar explanation holds for the last knot $s_{N/2-l_y}$. The elements $\bar{\psi}(s_{j_1})$ and $\bar{\phi}(s_{j_1})$ need not to be included because $w'(s_{j_1}) = w'(s_{N-j-1}) = w'(s_{N+j_1}) = w'(s_{2N-j_1}) = 0$. The modified expressions for $\mathbf{D}_l, \mathbf{D}', \mathbf{T}$ are given in the same way as for $\mathbf{S}_l$.

5 Multimode Waveguides

For a multimode waveguide as used in data communication, the waveguide frequency V could be very large (typically in the range of 10-100). In the Nyström method, the logarithmic parts are separated completely from the kernels such that the remaining parts are analytic (c.f. (11a)-(11d)). This splitting method is not good if V is too large as we shall explain next.

A physically correct eigenvalue P (for guided modes) must be a real number in the interval $(0, 1)$. In this case, h_1 is a real number and h_2 is an imaginary number and thus $h_2 = -i|h_2|$. But $J_n(-i|h_2|R) = \exp(in\pi/2)I_n(|h_2|R)$, where I_n is the nth order modified Bessel function of the first kind, and it increases exponentially when the argument becomes large. Therefore, the determinants of the coefficient matrices in (16) and (17) as the functions of P are oscillating around zero with amplitudes which are exponentially increasing when P goes from 0 to 1. This is very bad for root searching in the interval $(0, 1)$, and overflow can happen.

Actually, the kernels S_2, D_2 and the parts of the kernels D' and T which include h_2 decay exponentially as $|h_2|R$ becomes large because $H_n^{(2)}(-i|h_2|R) = 2i^{n+1}K_n(|h_2|R)/\pi$ where K_n is the nth order modified Bessel function of the second kind and it decays exponentially when the argument becomes large. By using the splitting method (11a)-(11d) (only $l = 2$ is concerned here), each of the functions that decay exponentially as $|h_2|R$ becomes large is separated into two parts that exponentially *increase* as $|h_2|R$ becomes large. Instead of doing this, there is a simple way to separate the logarithmic singularity partly from each of the kernels such that the two parts obtained (S_{21} and S_{22}, for example) decay exponentially as $|h_2|R$ becomes large and have continuous derivatives up to a certain order.

To realize this idea, what we can do is to replace $J_n(h_2R)$ in (12a)-(12d) by a truncation of the series expansion of $J_n(h_2R)\exp(ih_2R)$ multiplied by $\exp(-ih_2R)$. Assuming

$$J_n(z)\exp(iz) = \sum_{k=0}^{\infty} a_k z^k = \sum_{k=0}^{L} a_k z^k + O(z^{L+1}), \tag{30}$$

we define

$$cJ_n(z, L) = \exp(-iz)\sum_{k=0}^{L} a_k z^k. \tag{31}$$

It is obvious that $J_n(z) - cJ_n(z,L) = O(z^{L+1})$. Thus $cJ_n(z,L)$ has a very similar behavior as $J_n(z)$ as $z \to 0$ and decays exponentially as $|z|(z = -i|z|)$ becomes large. So, for the multimode waveguides, everything is the same except replacing $J_n(h_2R)$ by $cJ_n(h_2R,L)$ $(n = 0,1,2)$ where

$$cJ_n(z,L) = \exp(-iz)z^n \sum_{k=0}^{L-n} \sum_{m=0}^{[k/2]} \frac{1}{(m!)(m+n)!(k-2m)!2^{(2m+n)}}(iz)^k. \tag{32}$$

Remark: In the case of a non-smooth boundary, $S_{21}w'(s)$ and $S_{22}w'(s)$ etc. are no longer analytic. Therefore, we have not lost anything by using the new procedure.

6 Examples

To solve (21) numerically, we let P go from 0 to 1 with a step length dP. When both the real part and imaginary part of $|Q(P)|$ change their signs in one step, the Newton-Raphson method [11] is used to search the root in this interval as follows:

$$P^{(n+1)} = P^{(n)} - \frac{1}{\mathrm{tr}[Q^{-1}(P^{(n)})Q'(P^{(n)})]}, \quad n = 0,1,2,..., \tag{33}$$

where tr denotes the trace of a matrix, $Q' = \frac{dQ}{dP}$, and P^0 is the mid-point of the interval. The search can also be started from any initial guess $P^{(0)}$. The derivatives of the two coefficient matrices in (16) and (17) with respect to P can be easily derived and are not given here. Both circular and rectangular waveguides are computed. The symmetry property of the two waveguides is used in our calculations. All computations are done in double precision.

In the first numerical example, we compute the normalized propagation constants P for a circular step-index waveguide. The waveguide frequency V of a circular waveguide is defined by $V = ak(n_1^2 - n_2^2)^{1/2}$ where a is the radius of the circle. Table 1 shows the numerical results for the LP_{02} mode of a circular waveguide with $V = 5$ (there are totally four eigenmodes in this case). Here the notation LP_{mn}, where LP means "linearly polarized", designates modes of a step-index circular waveguide in the weakly guiding approximation. The subscripts m and n designate the circumferential order and the radial order of a mode, respectively, see [8] for details. The number of mesh points is $2N - 1$. The exact result is $P = 0.215425919556543$. The exponential convergence of the Nyström method is clearly exhibited for both methods.

Table 1: Numerical results for HE_{12} mode (circular)

	N	Re(P)	Im(P)
First	4	0.219878316109075	$-9.141104813018 \times 10^{-3}$
method	8	0.215426096200949	$-3.44135521 \times 10^{-7}$
	16	0.215425919556542	10^{-16}
	32	0.215425919556543	10^{-16}
Second	4	0.207654035803197	$8.470981562227 \times 10^{-3}$
method	8	0.215425666039999	$7.99659140 \times 10^{-7}$
	16	0.215425919556542	10^{-16}
	32	0.215425919556543	10^{-16}

We see that the two methods have almost the same accuracy for this eigenvalue. However, spurious modes are observed for the first method. For example, two spurious modes $P = (0.501768094105135, 4.311 \times 10^{-12})$ and $P = (0.8405304424586, 1.1 \times 10^{-15})$ are obtained for $V = 5$ and $(l_x, l_y) = (0, 0)$ when $N = 12$. The two roots shift to $P = (0.58323712650253, 10^{-16})$ and $P = (0.8737774555242, 10^{-16})$ respectively when $N = 24$. No spurious modes have been observed for the second method for $V = 5$.

In the second numerical example, we compute the normalized propagation constants P for a rectangular step-index waveguide. The waveguide frequency V of a rectangular waveguide is defined by $V = 2bk(n_1^2 - n_2^2)^{1/2}/\pi$ (cf. Fig.2). Table 2 shows the numerical results for the E_{42} mode of a rectangular waveguide with $V = 4$ and $a/b = 2$(there are totally 25 eigenmodes in this case). Here the notation E_{mn}, introduced by Goell [12], designates modes of a step-index rectangular waveguide in the weakly guiding approximation. The subscripts m and n designate the number of maxima in the x and y directions, respectively. The two techniques in Sections 4 and 5 have been used in this calculation. The two integers p and L, which occur in the definitions of $w(s)$ and $cJ_n(z, L)$, are both taken to be equal to 8.

We see that both methods converge very fast. There is no analytic solution for a rectangular waveguide. The perturbation method [13] gives $P = 0.602868$ for this mode. In our calculations of rectangular waveguides, no spurious modes have been observed for both methods.

In the third example, we compute the eigenvalues of all eigenmodes which are symmetric

Table 2: Numerical results for E_{42} mode (rectangular)

	N	Re(P)	Im(P)
First method	32	0.603584063946075	$1.61600034847 \times 10^{-4}$
	64	0.603065248419964	$-4.75137113 \times 10^{-7}$
	128	0.603066935219651	$-2.2637421 \times 10^{-8}$
	256	0.603066923582579	-8.2098×10^{-11}
Second method	32	0.599160032739276	$1.823943976376 \times 10^{-3}$
	64	0.603066819764827	$-2.317229633 \times 10^{-6}$
	128	0.603066924119400	-3.9233×10^{-11}
	256	0.603066922973223	1.49664×10^{-10}

with respect to the x-axis and y-axis ($l_x = l_y = 0$), of a rectangular waveguide with $V = 10$ and $a/b = 2$. There are totally 43 such modes. The integers p, L, N are taken as $8, 10, 160$, respectively. The length step dP in the root searching is taken as 0.0001. Figure 4 shows the numerical results for those eigenvalues, using the first method. Figure 5 shows the differences between the numerical results P_n and the results obtained by first order perturbation P_n^ϵ (cf. [13]). Figure 6 shows the relative differences between the numerical results and the first order perturbation results. The (absolute) differences between the first and second boundary integral methods, i.e. (6a)-(6b) and (7a)-(7b), are less than 10^{-6}. It is known that the perturbation method is less accurate for the eigenmodes which are near cut-off (i.e., P is close to zero). The reason is that a significant part of the modal power of a near cut-off eigenmode spreads into the cladding. This fact can be seen clearly in our calculations.

Our numerical method converges for even larger values of V. For example, the second method gives $P = (0.45446055, -1.8145042 \times 10^{-5})$ and $P = (0.15939511, -3.3134108 \times 10^{-5})$ for the $E_{5,27}$ mode and $E_{26,31}$ mode of a rectangular waveguide with $V = 36$ and $a/b = 2$, respectively (there are over 1000 modes in this case); p, L, N are taken as $8, 8, 256$, respectively, in this calculation. The perturbation method gives $P = 0.45446549$ and $P = 0.16068805$ for the two modes, respectively.

7 Concluding Remarks

The boundary integral formulation, combined with the Nyström integration algorithm, has been shown to be very efficient in the modal analysis of homogeneous dielectric optical

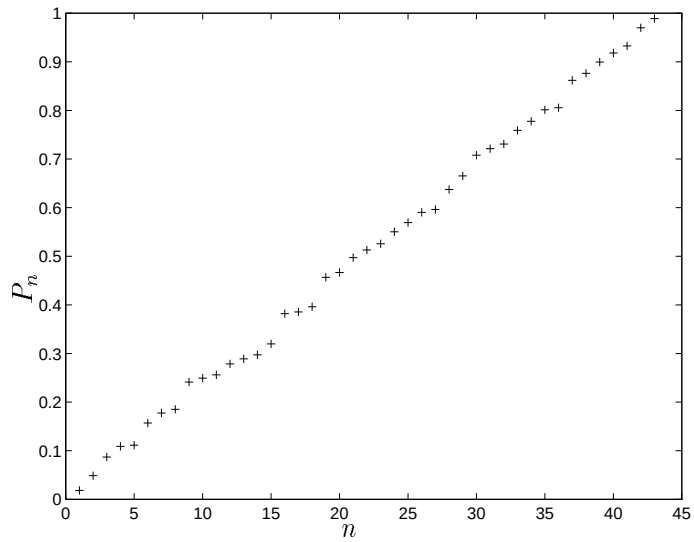

Figure 4: Eigenvalues of a rectangular waveguide with $V = 10$ and $a/b = 2$.

waveguides, with fast convergence and high accuracy. A key idea in the Nyström algorithm is to separate each of the non-analytic kernels into two parts: one includes the logarithmic singularity term and the other is analytic. This method of splitting kernels has been modified in this paper such that the numerical boundary integral method can be used to solve the optical waveguides with high waveguide frequencies or large waveguide cores (compared with the wavelength).

Two boundary integral formulations are presented, one of them is a Fredholm integral equation of the second kind and the other is a mixture of the second and first kind. Our numerical results show that these two methods are almost equally efficient in search of eigenvalues of homogeneous optical waveguides. Nevertheless, the integral equation of the second kind is more favorable because the other system has no rigorous mathematical theory of existence, and it also produces spurious modes

Finally, we point out that there is another way to derive a system of integral equations of the second kind for the boundary-value/eigenvalue problem (2a)-(2d). It is based on the mixed-layer potential representations of ψ in Ω and Ω^c instead of the Green's third identity. We assume

$$\psi_1(\mathbf{r}) = \int_{\partial\Omega} \frac{\partial G_1(\mathbf{r},\mathbf{r}')}{\partial n'} u(\mathbf{r}')dl' + \int_{\partial\Omega} G_1(\mathbf{r},\mathbf{r}')v(\mathbf{r}')dl', \quad \text{in } \Omega, \tag{34a}$$

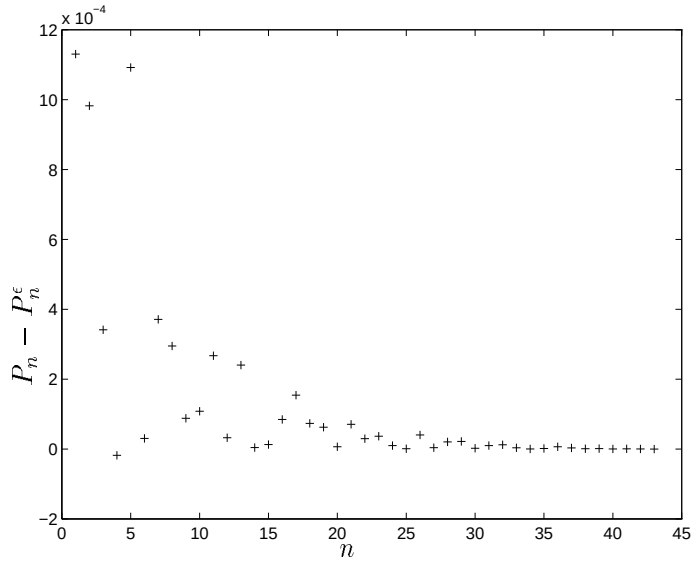

Figure 5: Differences between the numerical and perturbation methods.

$$\psi_2(\mathbf{r}) = \int_{\partial\Omega} \frac{\partial G_2(\mathbf{r},\mathbf{r}')}{\partial n'} u(\mathbf{r}')dl' + \int_{\partial\Omega} G_2(\mathbf{r},\mathbf{r}')v(\mathbf{r}')dl', \quad \text{in } \Omega^c. \tag{34b}$$

Using the boundary conditions

$$\psi_1 = \psi_2, \quad \frac{\partial \psi_1}{\partial n} = \frac{\partial \psi_2}{\partial n},$$

and the limiting behaviors of the single and double layer potentials when $\mathbf{r}$ goes to the boundary, we obtain

$$u(\mathbf{r}) + \int_{\partial\Omega} \frac{\partial}{\partial n'}(G_2 - G_1)u(\mathbf{r}')dl' + \int_{\partial\Omega} (G_2 - G_1)v(\mathbf{r}')dl' = 0, \tag{35a}$$

$$v(\mathbf{r}) - \int_{\partial\Omega} \frac{\partial^2}{\partial n \partial n'}(G_2 - G_1)u(\mathbf{r}')dl' - \int_{\partial\Omega} \frac{\partial}{\partial n}(G_2 - G_1)v(\mathbf{r}')dl' = 0, \tag{35b}$$

where $\mathbf{r} \in \partial\Omega$. This system is different from that of (7a)-(7b) only by two signs.

From the point of view of rigorous mathematics, we can only assert the following:

1. Any eigenmode must satisfy the integral equations (7a)-(7b), but this system may possibly have spurious modes (which can not be removed by mesh refinements).

2. Any solution of (35a)-(35b) is an eigenmode, although there may possibly be additional eigenmodes which are not given in the form (34a)-(34b).

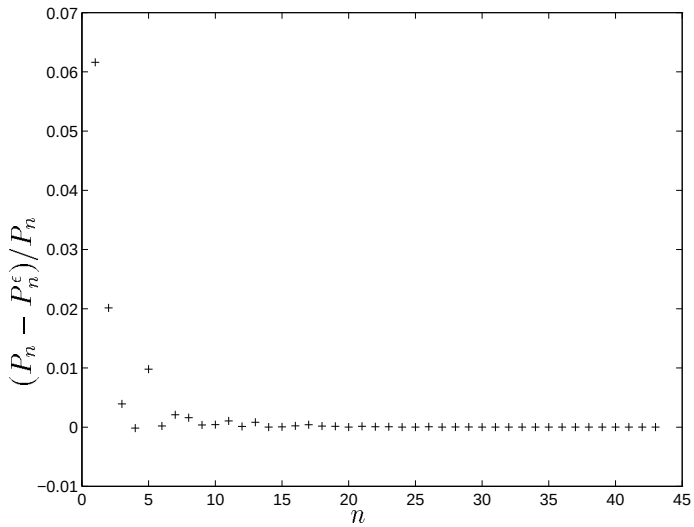

Figure 6: Relative differences between the numerical and perturbation methods.

However, in the circular case, $f_1(t) \equiv 1, f_2(t,\tau) = f_2(\tau,t)$, so that $(\mathbf{D}_2 - \mathbf{D}_1) = \mathbf{D}'$ and $\mathbf{T}, (\mathbf{S}_2 - \mathbf{S}_1)$ are symmetric. One can then prove that the determinants of the coefficient matrices of the two systems of boundary integral equations, (7a)-(7b) and (35a)-(35b), after discretization, are equal in this case. Our numerical calculations show that the two determinants are equal for other geometries also, including the rectangle and the geometries without symmetry.

References

[1] David Colton and Rainer Kress, *Integral Equation Methods in Scattering Theory*, John Wiley & Sons, 1983.

[2] P.K. Banerjee and R. Butterfield, *Boundary Element Methods in Engineering Science*, McGraw-Hill Book Company (UK) limited, 1981.

[3] C.C. Su, "A surface integral equations method for homogeneous optical fibers and coupled cross sections", *IEEE Trans. Microwave Theory Tech.*, MTT-33 (1985) 1351.

[4] E. Yamashita editor, *Analysis Methods for Electromagnetic Wave Problems*, Artech House Inc., 1990.

[5] J. Charles, H. Baudrand, and D. Bajon, "A full-wave analysis of an arbitrarily shaped dielectric waveguides using Green's scalar identity", *IEEE Trans. Microwave Theory Tech.*, MTT-39 (1991) 1029.

[6] R. Kress, *Linear Integral Equations*, Springer-Verlag, 1989.

[7] D. Colton and R.Kress, *Inverse Acoustic and Electromagnetic Scattering Theory*, Springer-Verlag, 1992.

[8] A.W. Snyder and J.D. Love, Optical Waveguide Theory, Chapman and Hall Ltd, 1983.

[9] O.D. Kellog, *Foundation of Potential Theory*, Dover Publication, New York, 1953.

[10] A.H. Juffer et. al., "The electric potential of a macromolecule in a solvent: a fundamental approach", *J. Comp. Phys.*, 97 (1991) 144.

[11] G. Chen and J. Zhou, *Boundary Elements Methods*, Academic Press, 1992.

[12] J.E. Goell, "A circular-harmonic computer analysis of rectangular dielectric waveguide", *The Bell System Technical Journal*, 9 (1969) 2132.

[13] A. Kumar, K. Thyagarajan, and A.K. Ghatak, "Analysis of rectangular-core dielectric waveguides: an accurate perturbation method", Opt. Lett., 1 (1988) 63.